

# Mixed EEG/MEG imaging: a way forward

R. Hasson  
Department of Physics  
The Open University  
Milton Keynes. MK7 7AA  
UK

## Introduction

It has been suggested that a combined Magnetoencephalography (MEG) / Electroencephalography (EEG) analysis technique would be a desirable aim. The main reason put forward in support of this suggestion is that there exist so called *silent* sources which are distributions of current which produce no external magnetic field. For example, it is well known that in the conducting sphere model of the brain a radial dipole is a silent source (see [17, 18]), but other arrangements also produce the same phenomenon [17]. It is also known that there exist arrangements of sources which produce no electrical potential differences at the surface of the head [18]. So the argument for a combined analysis system is that the electric potential and the magnetic field contain complimentary information about the primary source structure in the brain.

In [7] it was proposed that a combined method would be useful and a method for combining the two types of data was proposed which consisted of producing a minimum norm estimate for the combined signals. Whilst in [4] a three step method was suggested for mixed EEG/MEG analysis with a moving dipole algorithm. In this paper I will use variations of the probabilistic algorithm derived by Clark et al. [1, 3, 9].

One of the main disadvantages in working with EEG data is that any accurate model of the brain needs to know the conductivity profile of the head to a high degree of accuracy which is not so with MEG [8, 19]. This is a big problem since nobody knows the conductivity profile of the head to sufficient accuracy. This does not preclude a study into the possible advantages of such an approach as long as the signal data is generated by a computer rather than measured in reality. In this paper I will assume that an accurate model of the conductivities of the head will eventually be available and when this occurs the results from this study should remain valid. Having said that a totally realistic model is impossible, it remains to choose an appropriate model for the head which (hopefully) still retains the essential properties of a realistic model. It has been suggested [8] that a simple conducting sphere model [19] is adequate for MEG signals from superficial sources from the visual and auditory cortices which seems to be the case from out analyses of real data [10, 12]. This is

the model which I will use for computing magnetic fields. It is known however that this is not the case for electric potentials; so I decided to use a layered anisotropic concentric sphere model [14, 15].

The notation that I will use for both the MEG and EEG forward problems is as in figure 1 where  $\mathbf{r}$  is the position of the measurement point and  $\mathbf{r}_0$  is the position of the source dipole, of dipole moment  $M$ . There are  $N$  spheres of radii  $R_1, R_2, \dots, R_N$  of which  $R_1$  is the largest. The conductivities are assumed to be isotropic for the MEG forward problem, and the conductivity inside the  $i^{\text{th}}$  sphere will be denoted by  $\sigma_i$ . However the conductivities for the EEG forward problem are assumed to be  $\epsilon_i$  (resp.  $\eta_i$ ) for the radial (resp. tangential) conductivities inside the  $i^{\text{th}}$  sphere.

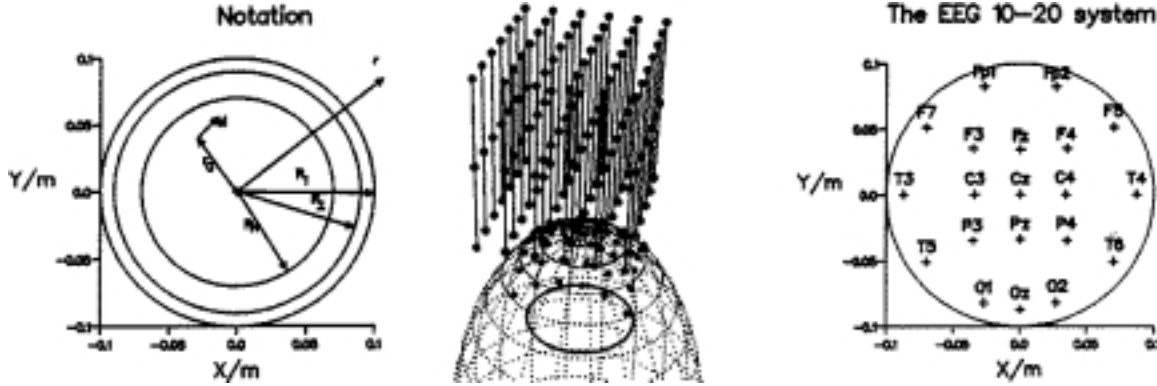


Figure 1: (left) The notation used for in the model for the both the MEG and the EEG forward problem.

(middle) The experimental geometry mostly used in this study. Note that the primary source space (the disk in which images are made) is reasonably deep into the sphere — this is precisely the region that MEG alone finds most difficult to localise a dipole source.

(right) The 10–20 system of EEG electrode placement (see [13]) which is used a calculation in the final section (the rest of the experimental geometry is as in the middle diagram).

In the following sections the magnetic field (resp. potential) is derived analytically for the MEG (resp. EEG) forward problem. The penultimate section contains a brief description of the inverse problem algorithm used (as derived in [1, 3, 9]). In the final section the results of this study into mixed EEG/MEG inversions is presented and some conclusions are draw about the feasibility of using this technique in practice.

## The MEG forward problem

From the quasi-static approximation to Maxwell's equations it is possible to derive Geselowitz' formula [5, 19]

$$\mathbf{B}(\mathbf{r}) = \mathbf{B}_0(\mathbf{r}) - \frac{\mu_0}{4\pi} \sum_{i=1}^N (\sigma_i - \sigma_{i+1}) \int_{S_i} \psi(\mathbf{r}') \mathbf{n}(\mathbf{r}') \times \frac{\mathbf{r} - \mathbf{r}'}{|\mathbf{r} - \mathbf{r}'|^3} dS_i$$

Where  $S_i$  is the surface of the sphere of radius  $R_i$  and  $\mathbf{n}(\mathbf{r}')$  is the unit normal to the surface  $S_i$  at  $\mathbf{r}'$  and  $\mathbf{B}_0(\mathbf{r})$  is the magnetic field that would be generated by the source current if it were in free space, viz.

$$\mathbf{B}_0(\mathbf{r}) = \frac{\mu_0}{4\pi} \int_{R^3} \mathbf{J}^i(\mathbf{r}') \times \frac{\mathbf{r} - \mathbf{r}'}{|\mathbf{r} - \mathbf{r}'|^3} d\mathbf{r}'$$

If we use the above formula to calculate the radial component of the magnetic field (i.e.  $\mathbf{B}(\mathbf{r}) \cdot \hat{\mathbf{e}}_r$ ) then we find that the sum over the potentials is zero since the normal to a sphere is radial. To calculate the other components of the magnetic field we use the magnetic scalar potential :

$$\begin{aligned} U(\mathbf{r}) &= - \int_0^\infty \nabla U(\mathbf{r} + t\hat{\mathbf{e}}_r) \cdot \hat{\mathbf{e}}_r dt \\ &= \frac{1}{\mu_0} \int_0^\infty \mathbf{B}_r(\mathbf{r} + t\hat{\mathbf{e}}_r) dt \\ &= \frac{1}{\mu_0} \int_0^\infty \mathbf{B}_0(\mathbf{r} + t\hat{\mathbf{e}}_r) \cdot \hat{\mathbf{e}}_r dt \\ &= \frac{1}{4\pi} M \times (\mathbf{r} - \mathbf{r}_0) \cdot \hat{\mathbf{e}}_r \int_0^\infty \frac{dt}{|\mathbf{r} + t\hat{\mathbf{e}}_r - \mathbf{r}_0|^3} \\ &= -\frac{1}{4\pi} \frac{M \times \mathbf{r}_0 \cdot \mathbf{r}}{F} \end{aligned}$$

where  $F = |\mathbf{r} - \mathbf{r}_0| \{ |\mathbf{r} - \mathbf{r}_0| \parallel \mathbf{r} | + (\mathbf{r} - \mathbf{r}_0) \cdot \mathbf{r} \}$ . Then we use the formula which defines the magnetic scalar potential (viz.  $\mathbf{B}(\mathbf{r}) = -\mu_0 \nabla U(\mathbf{r})$ ) to get the formula for the magnetic field to be :

$$\mathbf{B}(\mathbf{r}) = \frac{\mu_0}{4\pi F^2} [F \mathbf{M} \times \mathbf{r}_0 - ((\mathbf{M} \times \mathbf{r}_0) \cdot \mathbf{r}) \nabla F]$$

Note that the radius of the conducting sphere does not appear anywhere in the following formulae and so this model predicts the same results for any sphere that contains the source space and does not intersect the detector space. Note also that the conductivities also do not appear in this formula so the magnetic field is independent of them. This fact justifies the statement made in the introduction that the magnetic field measurements are less sensitive to the (unknown) conductivities of the various parts of the head.

## The EEG forward problem

In this section I will give a brief exposition of the EEG forward problem for a layered anisotropic spherically symmetric volume conductor, a more full account is contained in [14].

From the quasi-static approximation to Maxwell's equations it is easy to derive the following formula which expresses the electrical potential  $\psi$  in terms of the sources  $s$  and the conductivity  $\sigma$  :

$$\nabla \cdot (\sigma \nabla \psi) = s$$

With the model described in the previous section this equation becomes :-

$$\frac{1}{\eta} \frac{\partial}{\partial r} \left( r^2 \epsilon \frac{\partial \psi}{\partial r} \right) + \frac{1}{\sin \theta} \frac{\partial}{\partial \theta} \left( \sin \theta \frac{\partial \psi}{\partial \theta} \right) + \frac{1}{\sin^2 \theta} \frac{\partial^2 \psi}{\partial \phi^2} = \frac{r^2 s}{\eta} \quad (1)$$

In order to solve this equation, for the monopole source  $s = \frac{M_{\text{mon}}}{r^2 \sin \theta} \delta(r - r_0) \delta(\theta - \theta_0) \delta(\phi - \phi_0)$ , the following series is substituted into the previous equation.

$$\psi = \sum_{n=0}^{\infty} \sum_{m=0}^n \sum_{\alpha=0}^1 \frac{M_{\text{mon}} R_n(r_0, r) Y_{nm\alpha}(\theta_0, \phi_0) Y_{nm\alpha}(\theta, \phi)}{|Y_{nm\alpha}(\theta, \phi)|^2} \quad (2)$$

where the  $Y_{nm\alpha}(\theta, \phi)$  are spherical harmonics, defined by :-

$$Y_{nm\alpha}(\theta, \phi) = \begin{cases} P_n^m(\cos \theta) \cos m\phi & \text{if } \alpha = 0 \\ P_n^m(\cos \theta) \sin m\phi & \text{if } \alpha = 1 \end{cases}$$

where  $P_n^m(z)$  is the associated Legendre function. When the above substitution is made, the  $\theta$  and  $\phi$  dependencies are satisfied by general results about spherical harmonics, and it can be shown that equation 1 is satisfied if the function  $R_n(r, r_0)$  satisfies :

$$\frac{d}{dr} \left( r^2 \epsilon \frac{dR_n}{dr} \right) - n(n+1)R_n \eta = \delta(r - r_0)$$

This equation can be solved by a standard method of solving the corresponding homogeneous equation and then combining the two solutions:

$$R_n(r, r_0) = \frac{-1}{(2n+1)\epsilon_N B_N^{(2)}} \begin{cases} R_n^{(2)}(r_0) R_n^{(1)}(r) & \text{if } r \leq r_0 \\ R_n^{(1)}(r_0) R_n^{(2)}(r) & \text{if } r \geq r_0 \end{cases}$$

where the solutions of the homogeneous equations are :

$$R_n^{(i)} = A_j^{(i)} r^{\nu_j} + B_j^{(i)} r^{\nu_j} \quad \text{if } R_j \geq r \geq R_{j+1}$$

with  $A_j^{(i)}, B_j^{(i)}$  chosen to satisfy the boundary conditions and

$$\nu_j = \frac{1}{2} \left( -1 + \sqrt{1 + \frac{4n(n+1)\eta_j}{\epsilon_j}} \right)$$

When this equation for  $R_n(r, r_0)$  is substituted back into equation 2 the solution for a monopole source is found. In order to find the solution for a dipole we simply take the gradient with respect to the source point and then take the inner product with the dipole moment  $M$  :

$$\psi_{\text{dip}} = \sum_{n=0}^{\infty} \sum_{m=0}^n \sum_{\alpha=0}^1 \frac{Y_{nm\alpha}(\theta, \phi)}{|Y_{nm\alpha}|^2} M \cdot \nabla_0 [R_n(r_0, r) Y_{nm\alpha}(\theta_0, \phi_0)]$$

Now we can simplify the algebra at this point by rotating space so that the dipole lies on the z-axis (i.e.  $\theta = 0$ ) and is pointing in the xz-plane (i.e  $M_y = 0$ ). The first rotation can be effected by the matrix

$$\begin{pmatrix} \sin \phi & -\cos \phi & 0 \\ \cos \phi \cos \theta & \sin \phi \cos \theta & -\sin \theta \\ \cos \phi \sin \theta & \sin \phi \sin \theta & \cos \theta \end{pmatrix}$$

This matrix rotates the dipole moment  $M$  to get  $\bar{M}$  which then can be rotated by the following matrix to get the  $\bar{M}_y$  component zero.

$$\frac{1}{\sqrt{\bar{M}_x^2 + \bar{M}_y^2}} \begin{pmatrix} \bar{M}_x & \bar{M}_y & 0 \\ -\bar{M}_y & \bar{M}_x & 0 \\ 0 & 0 & \sqrt{\bar{M}_x^2 + \bar{M}_y^2} \end{pmatrix}$$

and the final formula for the potential for a dipole source is :

$$\psi_{\text{dip}} = \frac{-1}{4\pi} \sum_{n=1}^{\infty} \frac{R_n^{(2)}(r)}{\epsilon_N B_N^{(2)}} \left\{ M_z \frac{dR_n^{(1)}(r_0)}{dr_0} Y_{n00}(\theta, \phi) + M_x \frac{R_n^{(1)}(r_0)}{r_0} Y_{n10}(\theta, \phi) \right\}$$

The model parameters that I have used for the model calculations in this study were taken from [15] and can be described as follows :

shell	radius	conductivity	
		radial ( $\epsilon_i$ )	tangential ( $\eta_i$ )
skin	1.0	1.0	1.0
skull	0.92	0.004	0.04
fluid	0.88	3.0	3.0
brain	0.85	1.0	1.0

## The inverse problem

The inverse problem algorithm that I propose to use makes use of the *lead fields* of the detectors. These are implicitly defined over the source space  $Q$  to be the solutions of the following equation:

$$m_i = \int_Q \mathbf{L}_i(\mathbf{r}) \cdot \mathbf{j}(\mathbf{r}) d\mathbf{r} \quad (3)$$

where  $m_i$  is the measurement at the  $i^{th}$  detector generated by the current density distribution  $\mathbf{j}(\mathbf{r})$ . By solving the forward problem for an dipole source (as in the previous sections) we can evaluate  $\{\mathbf{L}_i(\mathbf{r})\}$  throughout  $Q$ .

It would be instructive if at this point some remarks were made about the shape of the lead fields of the detectors used since it is these that are used as our basis functions for the inverse problem (see figure 2). The key feature that should be noted from this figure is that the lead field for the EEG electrode is far more localised than the lead field of the MEG gradiometer.

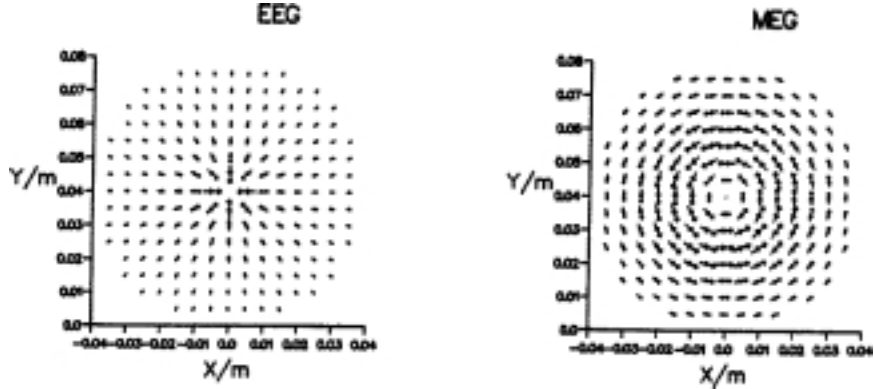


Figure 2: The patterns of the two types of lead field: EEG (left) and MEG (right)

The inverse problem algorithm that I will use is described in [1, 3, 9] and has the following main points

- It is assumed from the beginning that the current sources are confined within a small region of space  $Q$  (called the source space).
- The method does not allow sources beyond a certain strength (the exact value of which depends on a parameter of the method) and so biologically infeasible sources are excluded.
- Any information known *a priori* about the sources can be included in an easy way by coding it in a probability weight function  $w(\mathbf{r})$ .

- The formulation is in terms of linear combinations of the lead fields of the detectors. This is good because the current density is expressed in terms of functions which reflect the sensor sensitivities and thus problems due to the intrusion of ‘silent components’ [17, 18] into the solutions are avoided.
- Much of the computation is spent in the computation of the lead fields of the detectors which is independent of measurements and so can be separated out from the main part of the inverse problem.
- The method incorporates a regularisation parameter  $\zeta$  which smooths the image so that an acceptable picture results. This limits the detail that can be recovered and our ability to fit the data exactly (not a disadvantage in the presence of noise as it is futile to fit the data more accurately than its own standard deviation).

To be precise the inverse problem algorithm takes a set of measurements  $\{m_i \mid i = 1 \dots s\}$  and an *a priori* probability weight  $w(\mathbf{r})$  and produces the *expectation value* of the current density,  $\langle \mathbf{j}(\mathbf{r}) \rangle$ . The equations determining the algorithm are :

$$\begin{aligned} P_{ik} &= \int_Q \sum_s \mathbf{L}_i(\mathbf{r}) \cdot \mathbf{L}_k(\mathbf{r}) w(\mathbf{r}) d\mathbf{r} & (i, k = 1 \dots s) \\ \tilde{P}_{ik} &= \sum_{j=1}^s P_{ij} P_{jk} + \zeta P_{ik} & (i, k = 1 \dots s) \\ \tilde{m}_i &= \sum_{k=1}^s P_{ik} m_k & (i = 1 \dots s) \\ \tilde{m}_i &= \sum_{k=1}^s \tilde{P}_{ik} A_k & (i = 1 \dots s) \\ \langle \mathbf{j}(\mathbf{r}) \rangle &= \sum_{k=1}^s A_k \mathbf{L}_k(\mathbf{r}) w(\mathbf{r}) \end{aligned}$$

If an inversion is done with a mixed data set, say  $n$  MEG sensors and  $m$  EEG sensors, then there are two types of lead fields involved with grossly different magnitudes (since it is a lot easier for a source to produce a one volt potential difference than a one tesla magnetic field!). This leads to problems since an algorithm that is biased to produce small currents will automatically use only the EEG lead fields and so the contribution from the MEG is lost. There is a way round this however, if we decompose the  $(n+m) \times (n+m)$  matrix  $P$ , define above, in to the following blocks :-

$$\left( \begin{array}{c|c} A & C \\ \hline C^T & B \end{array} \right)$$

where  $A$  (resp.  $B$ ) is the  $n \times n$  (resp.  $m \times m$ ) matrix whose entries are the scalar products of the MEG (resp. EEG) sensors lead fields and  $C$  is the  $n \times m$

matrix whose entries are the scalar products of a lead field of an MEG sensor with the lead field of an EEG sensor. Then to balance the contributions of the EEG and MEG sensors the lead fields and data values of the MEG sensors are multiplied by a factor  $\gamma$  which is defined by :

$$\gamma = p_1 \times \sqrt{\frac{n \text{Tr} B}{m \text{Tr} A}}$$

and  $p_1$  is a parameter whose value determines the relative contributions of the MEG and EEG sensors.

## Conclusions

The inverse problem algorithm needs the lead fields to overlap significantly in order to effectively span the primary source space. So if we use widely spaced data the image that we get looks mainly the same as a single lead field of the detector(s) that are closest to the source as in the leftmost picture in figure 3. If we space the EEG detectors more closely then the EEG solution markedly improves.

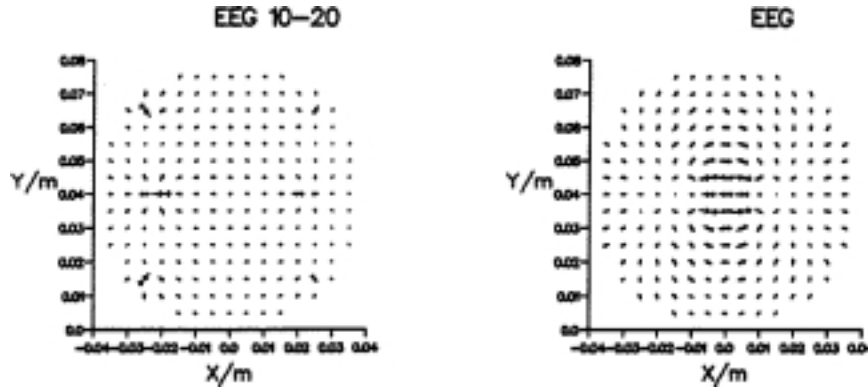


Figure 3: (left) An inversion done with the 10-20 system of electrode placement [13] which shows the effect of non-overlapping lead fields. (The source is a dipole at (0.0, 0.04) pointing parallel to the x-axis).

(right) A different experimental geometry 1 with overlapping lead fields (see figure 1) gives a better inversion on the same source.

It would appear that the EEG works quite well in that it localises to a very high degree a dipolar source, the reason that it can do this is that the phi functions are very sharp (see figure 2). This ability to localise a dipole source well is repeated if we add a large amount of noise to the data. In figure 4 we see that the EEG solution is more tightly localised around the correct region than

the MEG source. This is a disadvantage in the presence of modelling errors since this will introduce systematic errors into the EEG solution.

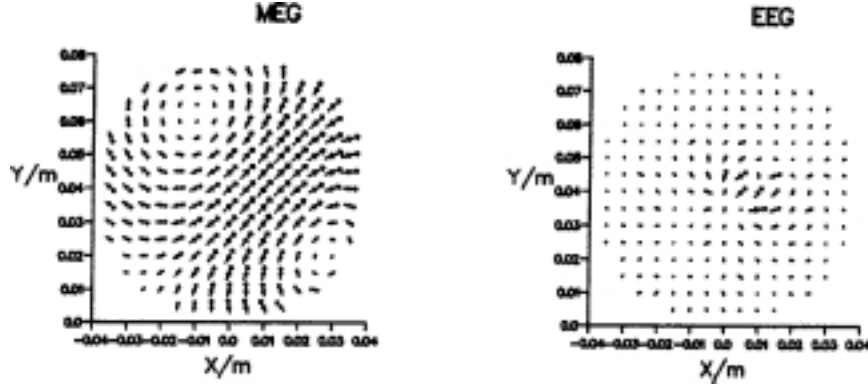


Figure 4: (left) An image produced by using data from the MEG gradiometers alone from a source located at  $(0.01, 0.04)$  with dipole moment  $(1.0, 1.0, 0.0)^T$  which has had noise added (equal to 20% of the peak to peak signal value). (right) An image produced by using the EEG electrode data alone from the same source.

The left hand diagram in figure 5 is the result of using a combination of the MEG and EEG data sets used to produce the images in figure 4. It can be seen that this image is even more localised than the EEG image and this is also reflected in fact that the correlation coefficient, which gives a measure of how well the solution fits the data, increases (from 88% to 92%). It is not known whether the combination of MEG and EEG data in the inverse problem algorithm described above is more robust to modelling errors than the using the EEG alone.

A method which is almost certainly more robust to modelling errors in the EEG inverse problem is a method in which the EEG data is just used as a guide for an inversion done with the MEG data only. The easiest way in which to do this is to first produce an image with the EEG data (or even better both the EEG and MEG data) and then use the image as an *a priori* probability weight for the inverse problem using the MEG data only. To be precise we use a probability weight  $w(\mathbf{r}_0)$  defined as follows:

$$w(\mathbf{r}_0) = |\mathbf{j}_{\text{EEG}}(\mathbf{r}_0)|^{p_2}$$

where the parameter  $p_2$  has been introduced so that we can alter the influence that the EEG solution has on the final image.

In conclusion, both the straightforward mixed algorithm and the two-step mixed algorithm developed in this study seem to be an improvement over using MEG alone in the localisation of deep sources. However, this is assuming

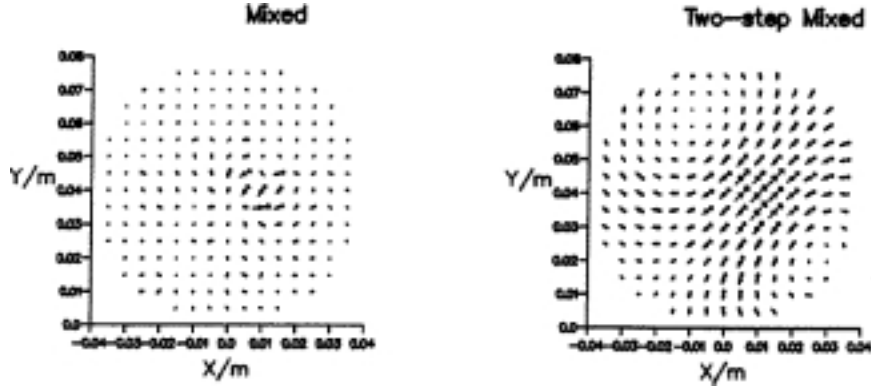


Figure 5: (left) An image produced by the mixed algorithm on the combined MEG/EEG data set used above with parameter  $p_1$  equal to  $\frac{1}{10}$ .  
 (right) The output of the two-step mixed algorithm with  $p_2$  equal to  $\frac{1}{3}$  and exactly the same data set.

that an accurate conductivity model for the head. One of the major questions that this study leaves unresolved is how sensitive are the results obtained to variations in the conductivities used in the model. I am undertaking a study of the dependencies of the algorithms described above on variations of the model parameters which I believe will show that the two-step algorithm is the most robust and is an improvement over using MEG alone.

## Acknowledgments

This work has been supported by a Science and Engineering Research Council award, under the Computational Science initiative. My thanks go to A.A. Ioannides and S.J. Swithenby for many helpful conversations regarding this present piece of work.

## References

- [1] C.J.S. Clarke, “Probabilistic Methods In a Biomagnetic Inverse Problem ”, *Inverse Problems* 5 999–1012, 1989.
- [2] C.J.S. Clarke, A.A. Ioannides and J.P.R. Bolton, “Localised and distributed source solutions for the biomagnetic inverse problem I”, In Proceedings of 7th International Conference on Biomagnetism (1989).
- [3] C.J.S. Clarke and B.S. Janday, “ Probabilistic Methods in a Biomagnetic Inverse Problem”, *Inverse Problems* 5, 483–500, 1989.

- [4] D. Cohen and B.N. Cuffin, "A method for combining MEG and EEG to determine the sources", Preprint.
- [5] D.B. Geselowitz, "On the magnetic field generated outside an inhomogeneous volume conductor by internal current sources", IEEE transactions on Magnetics, MAG-6 (2), 346–347, June 1970.
- [6] F. Grynspan and D.B. Geselowitz, "Model studies of the Magnetocardiogram", Biophysical Journal 13, 911–925, 1973.
- [7] M.S. Hämäläinen and R.S. Ilmoniemi, "Interpreting measured magnetic fields of the brain: estimates of current distributions", Preprint TKK-F-A559, Helsinki University of Technology, 1984. (submitted to IEEE, 1990).
- [8] M.S. Hämäläinen and J. Sarvas, "Feasibility of the homogeneous head model in the interpretation of neuromagnetic fields", Phys. Med. Biol. 32 (1), 91–97, 1987
- [9] A.A. Ioannides, J.P.R. Bolton and C.J.S. Clarke, "Continuous Probabilistic Solutions to the biomagnetic inverse problem", Inverse Problems 6 1–20, 1990.
- [10] A.A. Ioannides, J.P.R. Bolton, R. Hasson and C.J.S. Clarke, "Localised and distributed source solutions for the biomagnetic inverse problem II", In Proceedings of 7th International Conference on Biomagnetism (1989).
- [11] A.A. Ioannides, R. Hasson and J. P. R. Bolton, "Spatial and Temporal Evolution of Brain Activity", Open University video, July 1989.
- [12] A.A. Ioannides, R. Hasson and G. J. Miseldine, "Model-dependent noise elimination and distributed source solutions for the biomagnetic inverse problem", In proceeding of SPIE conference 1351 on, "Digital Image Synthesis and Inverse Optics", Ed. A. F. Gmitro, P. S. Idell and I. J. Lahaie. San Diego, July 1990.
- [13] H.H. Jasper, "The ten-twenty system of the international federation", EEG and Clin. Neuro. 10, 371, 1958.
- [14] J.C. de Munck, "The potential distribution in a layered anisotropic spheroidal volume conductor", J. Appl. Phys. 64 (2), 464–470, 15 July 1988
- [15] J.C. de Munck, "A mathematical and physical interpretation of the electromagnetic field of the brain", Ph.D. Thesis, University of Amsterdam, 1989.
- [16] J.C. de Munck and B.W. van Dijk, "Mathematical and physical aspects of volume conductor theory", preprint.

- [17] J.C. de Munck and B.W. van Dijk, “Symmetry considerations in the quasi-static approximation of volume conductor theory”, preprint.
- [18] B.J. Roth and J.P. Wilkswo, “Electrically silent magnetic fields”, Biophys J. 50, 739–745, October 1986
- [19] J. Sarvas, “Basic mathematical and electromagnetic concepts of the biomagnetic inverse problem”, Phys. Med. Biol. (32), 11–22, 1987.